

On Functional Segregation of fMRI-EEG derived Brain Connectomes



João Coelho (86448) and João Saraiva (86449)

Network Science - Second Project - 2020

ABSTRACT

The human brain comprehends specialized cortical regions that exchange information with each other. This results in these regions being divided into modules that function together in a combination of segregated (local) and integrated (distributed) processes. Hence, graph theory equips us with a toolbox to study these segregated and integrated processes. We analyzed one healthy subject brain connectome derived from the dual imaging technique fMRI-EEG, on a resting-state mode. The participation of nodes in exchanging information with other communities was found to be positively correlated to the rich club of the networks. The nodes with lower participation are thought to play a role in the network segregation, whether the nodes with high participation contribute to the network integration, such as the temporal poles and the parahippocampal gyri. As suspected, more segregation-contributing nodes were found in the high frequency EEG rhythms. Also, the so-called resting-state Default Brain Network was found inside a community.

Keywords: functional connectivity, fMRI, EEG, functional segregation, modularity, participation coefficient

1 INTRODUCTION

It is still today one of the biggest open questions in neuroscience how the complex topological properties of the human brain relate to its function. Over the last couple of decades, network science has provided us with the tools to create human brain models to better answer this wide question [1, 2]. Research has shown that brain networks show complex topological properties, such as, small-worldness at whole-brain and cellular scales [3, 4], existence of hubs over different frequency scales in fMRI and electrophysiological data, [3, 4], hierarchical modularity [5, 6], and rich-club organization [7]. Also, the presence of clusters and communities in functional connectomes suggests an organization of segregated neural processing [8]. Functional segregation of information flow in the human brain has been proved to be the mechanism that allows us to reconfigure the brain network dynamically and adaptively in response to the environment [9, 10]. And the participation of nodes in information flow between these communities is indicative of which nodes may contribute to segregation, and which nodes may contribute to integration of the network [8]. Inspired by these discoveries, in this project we propose to understand this mechanism using graph theory on a resting-state brain connectivity network of a healthy subject.

1.1 BOLD fMRI Signal

The data used was acquired from blood-oxygen-level dependent (BOLD) functional magnetic resonance imaging (fMRI). The BOLD signal comes from the change in blood flow (hemodynamic response, HDR) related to the energy used by brain cells, so it is considered an indirect measure of the brain neural activity. This signal lags

the neuronal electrical activity, since it takes a while for the vascular system to respond to the activity glucose demand [11]. This HDR imposes a fundamental limit on the time-precision of the acquired images and their sampling rate. For that reason, fMRI images are typically acquired at the shortest time of repetition (TR) of 1 second, as our data was. On the other hand, fMRI images show great spatial resolution down to the submillimeter scale, due to the signal's precise molecular source. Since the data was acquired in resting state, i.e., the subject was only looking to a wall, not performing any tasks, the fMRI signal should show the subject's baseline BOLD variance.

1.2 EEG Signal

Dual imaging modalities are a usual practice with fMRI, in particular with electroencephalography (EEG), in order to collect good temporal resolution information. Contrary to fMRI, which has an excellent spatial resolution, but a poor temporal resolution, EEG data lacks good spatial precision, but offers us excellent temporal insight. The EEG signal comes from the electrical voltage fluctuations of the brain cells, so it is considered a direct measure of brain neural activity [11]. The rhythmic activity of the EEG signal can be decomposed in different frequency bands, namely, the δ , θ , α , β , and γ rhythms, that are associated with different functions and locations.

2 RESULTS AND DISCUSSION

To be explicit, we will refer to the connectome as 7 independent networks. One holding the fMRI data, other holding the EEG broad-signal, and five holding the decomposition of the signal into the δ , θ , α , β , and γ rhythms (See Methods). There are also snippets on the margins to indicate which brain region is being referred on the text.

Table 1. Global properties of our networks, namely, average degree, $\langle k \rangle$, weighted average degree, $\langle k_w \rangle$, average clustering coefficient, $\langle C \rangle$, average path length, APL , network diameter, d , and network density, D . It also includes the clustering coefficient and average path length of the null models, $\langle C_{null} \rangle$ and APL_{null} , respectively.

Note: The edge values scale used in the fMRI matrix is different from the scale used in the EEG matrices, therefore the $\langle k_w \rangle$ absolute values cannot be directly compared between these two groups.

	fMRI	EEG					
		broad	δ	θ	α	β	γ
$\langle k \rangle$	33	23	25	23	24	22	22
$\langle k_w \rangle$	6.54	1.07	1.47	1.20	1.32	0.97	1.07
$\langle C \rangle$	0.67	0.58	0.52	0.55	0.57	0.55	0.57
$\langle C_{null} \rangle$	0.49	0.34	0.37	0.35	0.36	0.32	0.31
APL	1.51	1.70	1.65	1.71	1.71	1.73	1.71
APL_{null}	1.50	1.65	1.63	1.66	1.65	1.68	1.68
d	3	3	3	3	4	3	3
D	0.50	0.34	0.37	0.34	0.36	0.32	0.32

2.1 Global and Nodal Properties

Before diving into the neural segregation study, we performed some global analysis on the networks to have a general overview. Table 1 shows the average degree (unweighted and weighted), the average cluster coefficient, the average shortest path length, the diameter, and the density of our post-processed networks.

We built null models for each network (a random graph with the same degree distribution) and computed their average clustering coefficient, $\langle C_{null} \rangle$. According to the Erdős–Rényi model [12], the randomness of the null models leave them with a low clustering coefficient. As can be seen in Table 1, the $\langle C \rangle$ of each network was higher than the corresponding $\langle C_{null} \rangle$, suggesting a small-world property, described by the Watts and Strogatz model [13].

We also computed the APL for the null models, APL_{null} , which were very similar to those of the corresponding networks – see Table 1 – allowing us to conclude that to go from one node to another in our networks it takes a small path, suggesting again a small-word property.

This way, we can assume every network presents a small-world topology, as it has been heavily described in the literature for other brain connectivity networks. It is commonly thought that a small-world organization reflects an optimal balance of functional integration and segregation [14]. Furthermore, small-world networks are also abundant in hubs (nodes with a very high degree), as we shall discuss ahead.

As for the network densities, Table 1 shows these networks are not sparse as it would have been expected from small-world networks. Note that these densities are a product of the threshold we applied to the original ones. Regarding that, at first sight, we can assume good thresholds were applied, as we reduced the fMRI edges to half and all EEG networks present a reasonably similar density to be fairly compared.

2.2 Degree-Activity Correlation

From Table 1, we notice the unweighted average degrees of the EEG rhythms are very similar, although the low-frequency networks (δ , θ and α) have the highest $\langle k_w \rangle$ value, confirming the brain' resting state. This is not a significant increase in the $\langle k_w \rangle$ of the EEG- α network, which is in accordance with the fact that the subject had his/her eyes open during the procedure. If his/her eyes were to be closed, we would expect a much noticeable increase in the alpha power [15]. Also, we can notice the $\langle k_w \rangle$ of the EEG- β network is the lowest of them all, confirming the subject is not in an alert or attentive state [15]. The $\langle k_w \rangle$ of the EEG- γ network is the second lowest, confirming the subject is not performing any high-energy demanding tasks.

In the fMRI network, the frontal cortex is the lobe with higher intra-lobe $\langle k \rangle$ in each hemisphere, and between the left and right frontal cortices (2-3x higher than other lobes), but then it presents the lowest inter-lobe $\langle k \rangle$ in each hemisphere and between both hemispheres. Conversely, this situation was the opposite in the EEG- α network, where the frontal cortex presented the lowest intra-lobe $\langle k \rangle$ in each hemisphere, and between the left and right frontal cortices; and the highest inter-lobe $\langle k \rangle$ in the right hemisphere and between both hemispheres (exception in the left hemisphere). We verified the same in the parietal cortex. Laufs *et al.* have already reported a widespread negative correlation between fMRI and EEG- α data in the lateral frontal and parietal cortices, which are known to support attention and working memory [16].



2.3 Functional Hubs

Since the data was collected on a resting-state subject, we expect to see a high degree in the nodes of the so-called Brain Default Network (2008). The default network is a specific, anatomically defined brain system preferentially active when individuals are not focused on the external

environment, nor performing any demanding tasks [17]. It comprises the medial frontal cortex (mPFC), precuneus, posterior cingulate cortex (PCC), lateral parietal and temporal cortex, amygdala, and hippocampus. In 2014, the default network was revisited and three major functional hubs were said to hold the self-being information, namely, again the mPFC, the precuneus and the PCC [18], but also the angular gyrus. We introduce these regions below.

fMRI — In our fMRI network, the hubs correspond exactly to some of the mentioned regions, namely, the left and right superior temporal nodes, with a degree of 44 and 42, respectively. The left and right temporal pole nodes were also considered hubs, with a degree of 41 and 37, respectively. The left and right posterior cingulate nodes, corresponding to the PCC, are also hubs, with a degree of 43 and 41, respectively. The PCC has been implicated as a neural substrate for human awareness in numerous studies, and a tendency to functional segregation between memory and pain components, where memory activation is predominant in the caudal part and pain in the rostral part of the PCC [19]. The left parahippocampal node is also a 40 degree hub. Corresponding to the mPFC, the left and right superior frontal nodes were also considered hubs, with a degree of 38 both. All these nodes are connected to more than half of the network.

EEG — Regarding EEG, different rhythm networks revealed almost the same hubs, but with different degrees. For instance, for all rhythms, the left and right parahippocampal nodes were considered as hubs having a degree ranging from 34 to 41, except for the β and γ rhythms; in the β rhythm only the left one was considered a hub, just like in fMRI, with a degree of 42; and in the γ rhythm none was considered a hub. The precuneus and some nodes from the lateral temporal lobe and from the mPFC (superior frontal and medial orbitofrontal nodes) were also considered as hubs, except for the γ rhythm. Contrasting with the others, in the EEG-broad and EEG- γ networks, the left and right supramarginal nodes, and the right inferior parietal node were hubs (38, 44, 42, in the γ rhythm, respectively), which are the nodes corresponding to the left and right supramarginal gyrus, and the right angular gyrus, respectively. The angular gyrus is predicted in the default network, playing a role in integrating perception, attention, and spatial cognition, which functions positively correlated with the γ frequency [18].

Right Insula — The right insular cortex (right insula node) was considered a very high degree node in the δ , θ , and γ rhythm EEG networks, with a degree of 37, 35, and 43, respectively. The insular cortex can be found folded deep within the lateral sulcus. As for the left insula node, it is in every rhythm one of the four lowest degree nodes. Why is that? Specifically, the anterior insula is regarded as part of the limbic system, being involved in many processes of emotion, but also in the interoceptive awareness

of body states. It is believed the insula in the right hemisphere is more developed in humans than in other animal species, and that is considered an evolutionary trait that allows us to read the state of our bodies better than any other mammal [20, 21]. Also, only in the insula (and anterior cingulate cortex) we can find a type of neurons called the von Economo neurons (VENs), also product of evolution in humans and great apes, that with their very elongated axons can connect the insula to various parts of the brain, which is an essential attribute for its higher functions [20]. That associated with the selective role of the right anterior insula might be the reason why only the right insula node is the second highest degree hub in the EEG-broad network ($k = 44$).

2.4 Communities and Modularity

More sophisticated measures of segregation are dependent on the presence of densely interconnected regions, which is known as the network modular structure [22]. There are a number of algorithms that can partition the networks in communities, and we compared some of them through a quality function called modularity. Modularity, $Q \in [-0.5, 1]$, is the fraction of edges that fall within the communities minus the expected fraction if edges were distributed at random. If $Q > 0$, then the number of edges within groups exceeds the number expected on a random scenario. Below we present the results of community partitioning using the Louvain, Spinglass, Walktrap, Girvan-Newman, and Infomap algorithms.

2.4.1 Louvain-derived communities

The Louvain algorithm (Blondel *et al.* 2008) maximizes Q for each community, in the local moving of nodes phase and in the aggregation phase. In the first, individual nodes are moved to the community that yields the largest increase in Q . In the second, an aggregate network is created based on the partition obtained in the first phase. Each community in this partition becomes a node in the aggregate network. The two phases are repeated until the Q cannot be increased further [23]. Table 2 presents the number of communities found by the Louvain algorithm in every network, $\#C$, as well as each respective Q .

Table 2. Number of communities and modularity found by the Louvain algorithm for all networks.

	fMRI	EEG				
		broad	Δ	θ	α	β
#C	3	4	4	4	4	5
Q	0.35	0.21	0.20	0.21	0.19	0.22

This algorithm along with the Spinglass were the ones that yielded better contextualized results. In the fMRI network, one community in particular includes the nodes of the Default Network, namely the posterior cingulate, the precuneus, the superior frontal, the medial orbitofrontal,

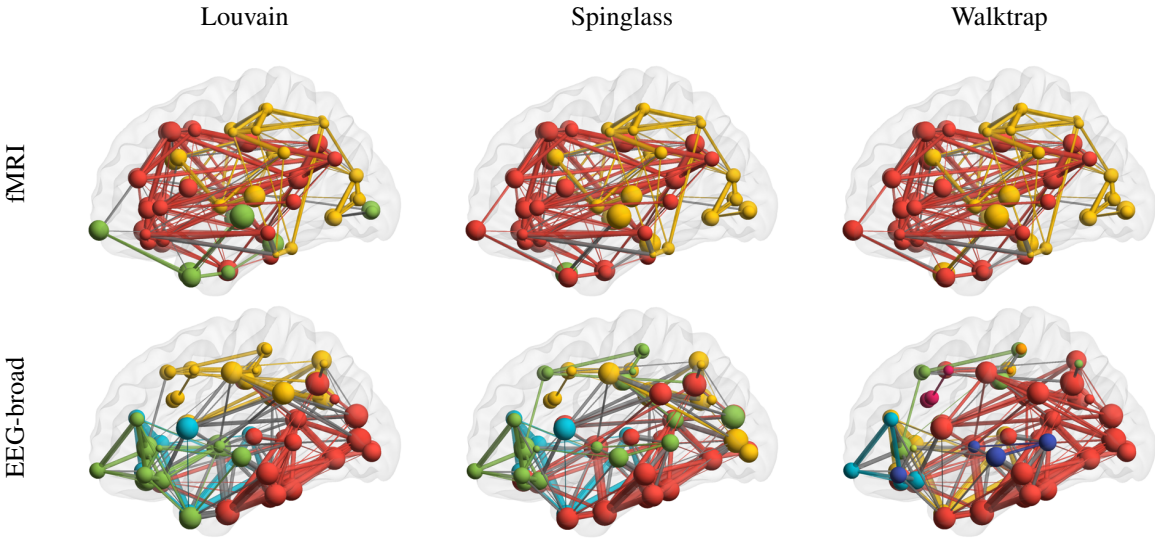


Figure 1. Whole-brain left sagittal views of the community divisions. Communities are divided in different colors. Node size represents their weighted degree, and edge size the weight of each link. For better visualization, the networks were drawn with 0.1 sparsity. Top stride: community division for the fMRI network performed by three algorithms: Louvain, Spinglass, and Walktrap. Bottom stride: community results for the EEG-broad network also performed by those three algorithms.

the inferior parietal, and the middle and inferior temporal nodes. But in the EEG-broad network, that is not the case. Instead, in Figure 1 we see a very boundary-clear community – the yellow one – comprising the superior nodes; and a red community comprising the posterior inferior nodes. The green and blue communities concentrate more ventral nodes from the left and right hemispheres, respectively. In fact, in the EEG rhythm networks, the communities were divided most of the time between the two hemispheres. For instance, in the EEG δ rhythm network, the yellow and red communities include the caudal, respectively, left and right nodes (Figure 2). The same applies to the green and blue communities, which include the rostral, respectively, left and right nodes.

2.4.2 Spinglass-derived communities

The Spinglass algorithm (Reichardt and Bornholdt 2006) relies on an analogy between a very popular statistical mechanic model called Potts spin glass, and the community structure. The community structure of the network is interpreted as the spin configuration that minimizes the energy of the spin glass with the spin states being the community indices. By applying the simulated annealing optimization technique on a model like this it's possible to optimize the modularity [24]. Table 3 presents the number of communities found by the Spinglass algorithm in every network, $\#C$, as well as each respective Q ; which yield very similar values to those in Table 2.

As we can see from Figure 1, the green community found by the Louvain algorithm is no longer a considerable community in the Spinglass division, because it only has one node. This node gets assigned to the yellow

Table 3. Number of communities and modularity found by the Spinglass algorithm for all networks.

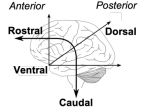
	fMRI	EEG				
		broad	Δ	θ	α	β
#C	3	4	3	4	4	5
Q	0.34	0.20	0.20	0.21	0.20	0.22
						0.22
						0.22

community by the Walktrap algorithm.

In the EEG-broad network, the red and blue communities are very identical to the division achieved by the Louvain, but some nodes of the green and blue communities got interchanged. In the EEG- δ network, Spinglass found only 3 communities, making a pretty good division between left (yellow) and right (red) hemispheres (Figure 2). One thing to notice in the δ and α rhythms is that the two frontal poles belong to the yellow community, which in the EEG- δ network concentrate more nodes in the posterior left side, but in the EEG- α network concentrate more nodes in the posterior right side. In the γ rhythm, the division was almost identical to the one found by Louvain, except the four purple nodes (posterior cingulate and paracentral) that were assigned to the yellow and blue communities, respectively, in the Spinglass division.

2.4.3 Walktrap-derived communities

The Walktrap algorithm (Pons and Latapy 2005) is based on random walks. The general idea is that if random walks are performed on the graph, then the walks are more likely to stay within the same community because there are only a few edges that lead outside a given community. It runs short random walks and uses the results of these to merge separate communities in a bottom-up approach [25].



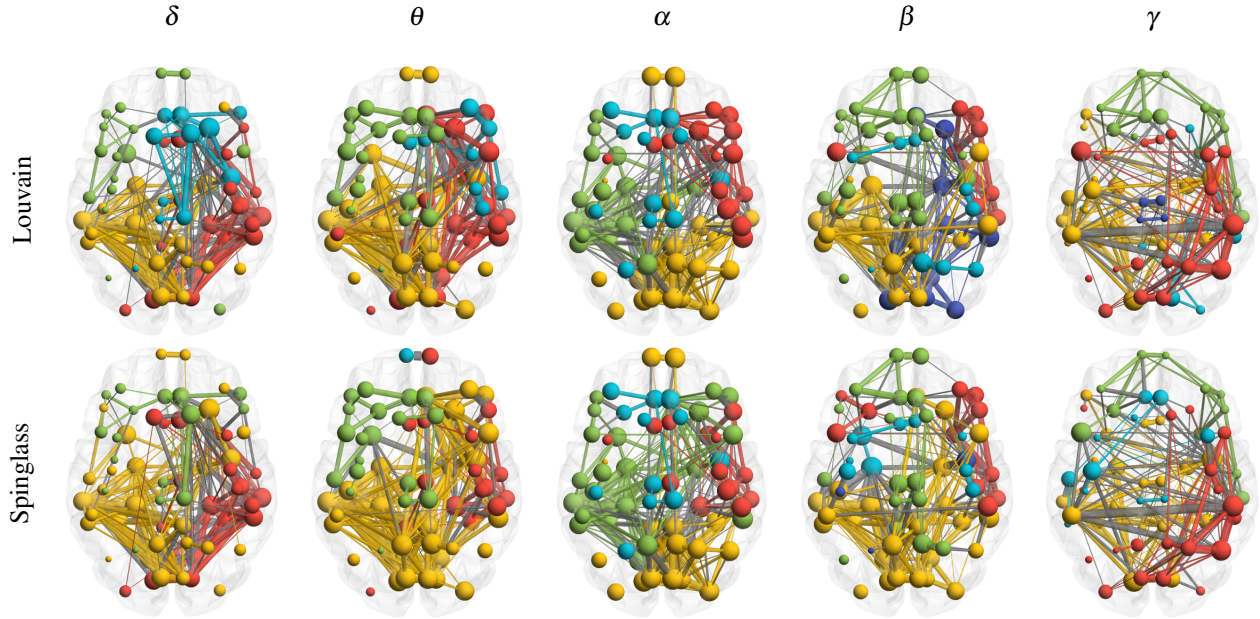


Figure 2. Whole-brain top axial views of different community division algorithms. The communities are divided in different colors. Node size represents their weighted degree, and edge size the weight of each link. For better visualization, the networks were drawn with 0.1 sparsity. Top stride: community results of the Louvain algorithm on the different EEG rhythm networks. On the bottom stride, there are the results achieved by the Spinglass algorithm on the same networks.

As aforementioned, the Walktrap algorithm performed more reasonably than the Spinglass in the fMRI network, dividing all nodes into two communities, with a modularity $Q = 0.343$, which is higher than $Q = 0.341$ in the Spinglass division. Although the two communities intersect, it is clear from Figure 1 the red community concentrates more nodes on the anterior side, and the yellow community concentrates more nodes on the posterior side. The Louvain algorithm segregated some inferior/caudal nodes in the green community, which is something to consider. The Walktrap algorithm performed more poorly in the EEG rhythm networks, with $0.10 < Q < 0.15$, except in the θ rhythm, which suggests a division much like the one achieved by the Spinglass in the θ rhythm as well, but with a lower modularity of $Q = 0.18$.

2.4.4 Other algorithms

We also tried the Girvan–Newman algorithm (2002), which detects communities by progressively removing the "most valuable" edge from the original graph, traditionally the edge with the highest betweenness centrality, at each step. As the graph breaks down into pieces, the tightly knit community structure is exposed [22]. For the EEG networks, this algorithm was not successful, obtaining modularities < 0.002 and in some cases negative. This is due to the fact that the edge betweenness centrality was found to be a poor metric for these networks. But for the fMRI, it divided the network in 4 communities with a modularity of $Q = 0.26$. Albeit with much lower modularity than the previous algorithms, the division was similar to

the one achieved by the Walktrap algorithm. The lower modularity is explained by a much bigger interception of the yellow and red communities, and also by two new one-node meaningless communities.

The Infomap algorithm (Rosvall and Bergstrom 2008), based on information theory, uses the probability flow of random walks on a network as a proxy for information flows in the real system. It decomposes the network into modules by compressing a description of the probability flow [26]. For the EEG networks, this algorithm was also not successful obtaining always just one community, hence not performing a division. But in the fMRI network, the result was pretty satisfactory, dividing the network in 3 communities, very similar to those of Louvain, also with a very similar modularity of $Q = 0.34$.

2.5 Inter-community Connectivity

On a functional brain connectome, a good measure of centrality may not always be the simple degree centrality, when we want to access how information flows between the communities. Functional central nodes are those who *participate* in many inter-community connections within the network, and consequently act as important controls of information flow. The participation coefficient (PC) is used to access the diversity of inter-community connections of individual nodes [27]. The complementary within-module degree (wMD) z-score is a localized, within-module version of degree centrality [27]. Based on that, one can classify within-module hubs (wMD z-score $> +1$) as provincial hubs, if they have a low participation

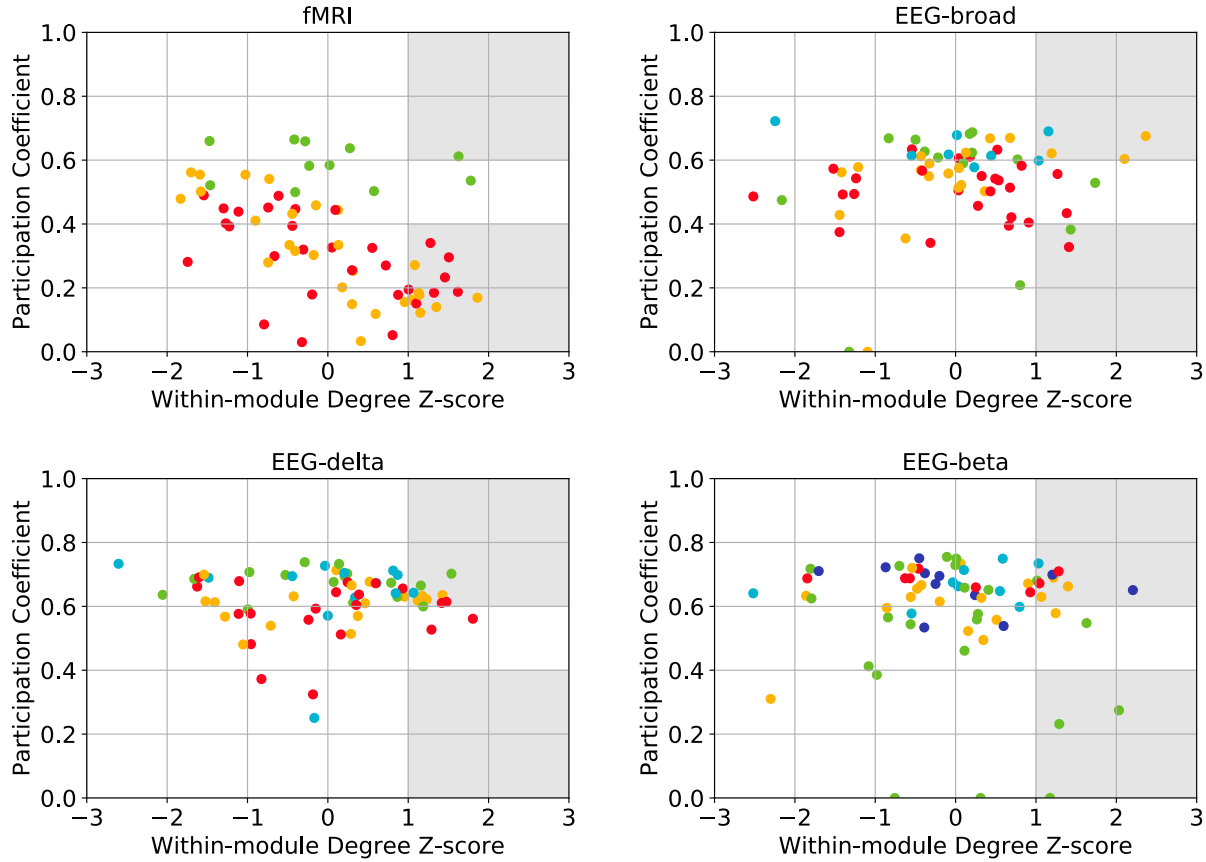


Figure 3. Participation Coefficient (PC) in function of the within-module Degree (wMD) z-score of all nodes in the fMRI network (top left), the EEG-broad network (top right), the EEG- δ network (bottom left), and the EEG- β network (bottom right). These two metrics were computed based on the Louvain community division. The node colors are the same used in Figures 1 and 2 and represent which community each node belongs in the Louvain community division. The nodes inside the gray areas are considered connector hubs ($PC > 0.6$) or provincial hubs ($PC < 0.4$).

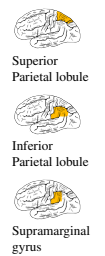
coefficient ($PC < 0.4$); or as connector hubs if they have a high participation coefficient ($PC > 0.6$). The tuple (wMD z-score; PC) will be used below to indicate the pair of values of each node.

Figure 3 presents the wMD vs. PC plots of some of the networks divided into communities by the Louvain algorithm. In the fMRI network, the right temporal pole from the green community was considered a connector hub (1.63; 0.61), since it connects directly with the red and yellow communities and is the highest-degree hub of its community. This way, it plays an important role in the facilitation of inter-modular integration [27]. Also, every node in the green community has a high PC. On the other hand, all the other nodes included in the bottom-right gray area are considered provincial hubs. These nodes are likely to facilitate modular segregation, by being the principal *distributors* of information inside their module, but *not participating* in many inter-modular connections. The right insula is one of these nodes.

The PC was originally proposed for metabolic networks, so it would *a priori* fit better on fMRI networks than EEG networks, since the fMRI BOLD signal is metabolically-driven. Nevertheless, some studies have

used this metric to evaluate EEG data [28, 29], and so will we. In the EEG-broad network, there are even two nodes that can't communicate directly with other communities. In this network, the connector hub with the highest PC is again the right temporal pole ($PC = 0.69$) that belongs to the blue community. It is a connector hub mostly due to the contribution of the β frequency, because it is also considered a connector hub in EEG- β network. The right superior (1.20; 0.62) and inferior (2.10; 0.60) parietal nodes and the right supramarginal node (2.37; 0.68) were also considered connector hubs. Recall that the inferior parietal node includes the angular gyrus reported in the Default Network. These three are connector hubs mainly due to their connectivity in the γ frequency.

Contrasting with the high frequency rhythms (β and γ), the δ , θ , and α rhythms did not contribute with provincial hubs to the EEG network. Meaning that the low frequencies facilitate more integration, than segregation of the brain. In fact, the EEG- δ network had the highest number of connector hubs, including the left temporal pole node (1.54; PC 0.70). The left (1.17; 0.63) and right (1.42; 0.61) fusiform nodes, and the right parahippocampal node (1.48; 0.61) are also connector hubs in this network.



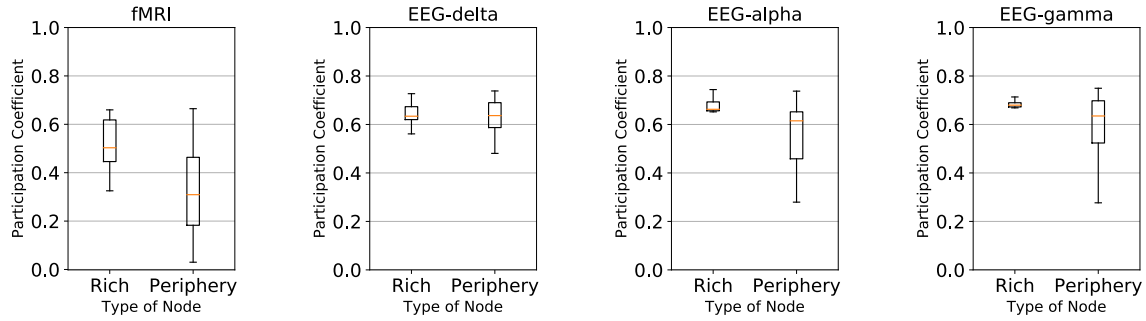


Figure 4. Participation Coefficient (PC) of nodes according to their relationship to the rich club in the fMRI, EEG- δ , EEG- α , and EEG- γ networks (from left to right side). Nodes can either belong to the Rich club or to the Periphery.

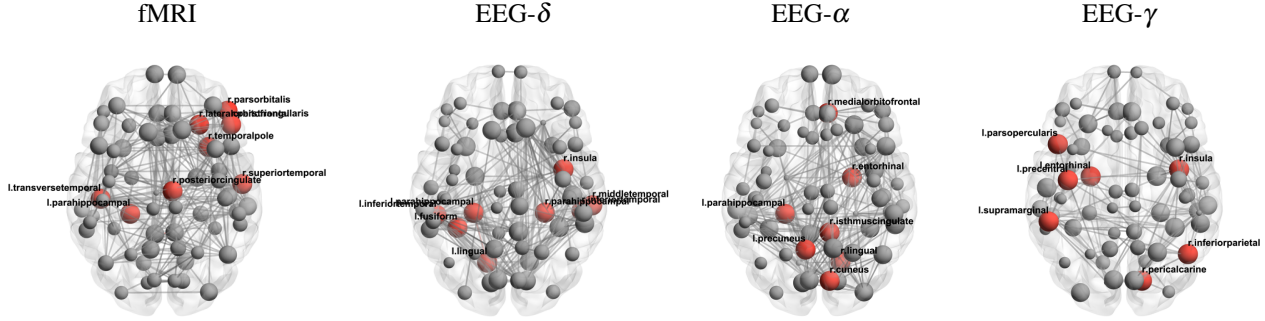


Figure 5. Whole-brain top axial views of the rich club nodes (in red) present in the fMRI, EEG- δ , EEG- α , and EEG- γ networks (from left to the right side). The rich club nodes' names correspond to the nearest text label. Node size represents their unweighted degree. For better visualization, the networks were drawn with 0.1 sparsity.

We can notice in the EEG- β network, that all red and blue nodes have high PC. Particularly, the red community is all contained in the right hemisphere and the blue community nodes with a wMD z-score > 0 are from the right hemisphere, suggesting more participation on the right hemisphere for higher frequencies, contrasting with more participation on the left hemisphere for lower frequencies. In fact, the three provincial nodes are from the left hemisphere and from the green community. This scenario facilitates the segregation of the EEG- β network into one more community than the low frequency EEG networks.

2.6 Rich Clubs

Some authors have tried to correlate the rich club organization of brain connectomes with the nodal participation coefficients [30]. As such, we conducted the same analysis on our networks. Rich club analysis aims to detect whether or not the high degree nodes of a network are well connected between themselves. If a node doesn't belong to the rich club, it is said to be a periphery node. The number of nodes in the rich club of each network, $\#R$, and their respective minimum degree, k_{rich} , is depicted in Table 4. These results enforce the rich-club organization reported in human brain connectomes.

As we can see from Figure 4, for each network, the rich club nodes have a higher participation coefficient than the periphery nodes. This means that rich club nodes tend to have connections more distributed among all communities. The quartile interval of the rich club is much smaller than

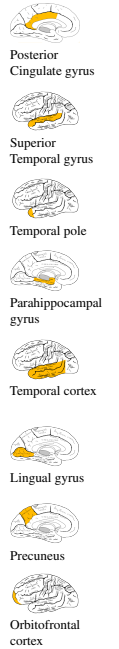
Table 4. Number of nodes and their minimum degree in the rich club of all networks.

	fMRI	EEG				
		broad	δ	θ	α	β
#R	8	5	8	11	7	9
k_{rich}	40	38	37	35	39	33
						34

that of the periphery nodes in the EEG- α and EEG- γ networks.

In Figure 5 we can see that the right posterior cingulate, the right superior temporal, the right temporal pole, the left parahippocampal and the left traverse temporal nodes belong to the fMRI network rich club. Notice this is a sub-list of the previously reported functional hubs and a sub-list of the described Default Network. While the two-hemisphere pairs make up these lists, the rich club includes only one node of one side from each pair. The left parahippocampal node also belongs to the rich club of the EEG- δ and EEG- α networks. The left lingual node belongs to the EEG- δ rich club, but the right analog belongs to the EEG- α rich club. The lingual gyrus has nothing to do with speech; instead plays a role in vision processing.

The left precuneus and the medial orbitofrontal nodes from the Default Network also belong to the EEG- α rich club. Regarding the right insula, it belongs to the rich club of the EEG- δ and EEG- γ networks. All these nodes contribute to the integration of the brain while resting at different activity frequencies.



3 CONCLUSIONS

Simple measures of segregation look for the presence of triangles in the network. The *rationale* is: the more clusters, the more locally segregated is the network. We can confirm from Table 1, either using fMRI or EEG, that our brain connectome presents a considerable number of clusters, therefore following evidence reported by other authors [5,6]. More complex measures of segregation take into account the precise location of the segregated regions, their size and their composition. The Louvain method has presented itself as the more accurate community division algorithm for our connectome, confirming the modular structure of our brain connectome either with fMRI or EEG data, as referenced in the literature [5,6].

Nonetheless, we should not forget each of these imaging techniques is used with different purposes to answer different questions. Being so, they complement each other, not substitute. That becomes clear when obtaining different results in the different networks for the participation coefficient to determine which nodes contribute more for segregation. We found that even in the different EEG rhythms, the nodes participation in the integration of the network varies. Specifically, in resting-state, the low frequency rhythms present more connector hubs, facilitating network integration; whereas the high frequency rhythms present more provincial hubs, facilitating network segregation. We also showed with data from both imaging techniques that, in this subject, the right temporal pole is one of the main integrator nodes in the connectome.

Future work should be directed in two routes. One in understanding the role of the Brain Default Network in neural functional segregation [31]. And another in performing the same study in the original dynamic connectomes.

4 METHODS

Data Acquisition. The data comes from subject 1 of the data set 4 of the project [32]. One run of 8 minutes resting-state simultaneous EEG-fMRI was acquired. The fMRI data was acquired in a 7T setup and obtained at a TR = 1s, TE=25ms, 69 slices, 220x220mm FOV, voxel size 2.2 x 2.2 x 2.2 mm, and a total of 480 volumes. The subject was with eyes open, fixating on a small red cross presented on a grey background. The EEG data was acquired using two 32-channel setups and a 63-electrode cap, plus reference, and one ECG electrode to reduce artifact contributions. Only 59 electrodes served to EEG recording, the remaining to motion artifact sensors.

Brain parcellation. The fMRI voxels parcellation was done into 86 regions according to the Desikan atlas [33], from which we only used the 68 cortical ones (excluding the subcorticals). Hence, the connectomes are to have 68 nodes. The EEG data was source reconstructed in order to have the time series associated to the same brain regions of the fMRI data, instead of having them associated with the electrodes, which may detect spatially overlapping signals and are generally not aligned with boundaries of fMRI regions [8].

Pre-processing. The connectivity matrices were 68x68x400, where 68 is the number of considered brain regions and 400 is the number of time points considered (1 per second). There were created 6 EEG connectivity matrices (broad signal, delta rhythm, theta rhythm, alpha rhythm, beta rhythm, and gamma rhythm) and 1 fMRI connectivity matrix. The fMRI and EEG matrices are relative to dynamic functional connectivity. The fMRI connectivity was computed with the phase coherence based on the Hilbert transform. And the EEG connectivity was computed with the imaginary part of coherency, averaged in windows of 4 seconds [34].

Static Connectome Construction. From the received connectivity matrices (68x68x400) we removed the first 3 time points of the fMRI connectivity matrix, and the last 3 time points of the EEG connectivity matrices, because the fMRI signal is 3 seconds delayed from the EEG signal, due to the intrinsic HDR mentioned in the Introduction. To obtain a static connectome (in time) an average over all the time points was performed in all connectivity matrices, ending up with static connectivity matrices (68x68).

Thresholding and Binarizing. Brain connectomes are often reduced to a sparse binary undirected form, through thresholding, binarizing, and symmetrizing [8]. Weak and non-significant links may represent spurious connections. These links tend to obscure the topology of strong and significant connections and as a result, are often discarded. In the fMRI matrix, all self-connections or negative connections (such as functional anticorrelations) were removed from the networks (set to zero) prior to analysis. For the EEG matrices, the choice of a fixed threshold for the connectivity matrices is usually based on the question(s) there are to be answered, and typically it requires very educated guesses. We used as thresholds the mean of connectivity values, being 0.0328 for the EEG-broad matrix, 0.0420 for the EEG- δ matrix, 0.0336 for the EEG- θ matrix, 0.0365 for the EEG- α matrix, 0.0301 for the EEG- β matrix, and 0.0328 for the EEG- β matrix. We also processed a binarized version of all the matrices, where each connectivity value > 0 is set to 1. In other words we kept two versions of the connectome, one with unweighted edges, and another with weighted edges. The weight of the edges is important in some topology metrics, to serve as function of connection strength [8].

Basic Measures. Being V the set of N nodes in the network and A the adjacency matrix, the degree of node i , k_i , is the number of edges connected to i . The shortest path length between nodes i and j is given by d_{ij} , where $g(i \leftrightarrow j)$ is the shortest path between i and j . The diameter of a network is the number of nodes of the longest path d_{ij} . The clustering coefficient of a network is given by C , where t_i is the number of triangles around i . And the density of a network is given by D , where E is the number of edges.

$$k_i = \sum_{j \in V} a_{ij} \quad d_{ij} = \sum_{uv \in g(i \leftrightarrow j)} a_{uv} \quad D = \frac{2E}{V(V-1)} \quad C = \frac{1}{N} \sum_{i \in V} \frac{2t_i}{k_i(k_i-1)}$$

Modularity. Modularity, Q , is the fraction of the edges that fall within the given communities minus the expected fraction if edges were distributed at random. It is defined as follows [35]:

$$Q = \frac{1}{2m} \sum_{vw} \left(A_{vw} - \frac{k_v k_w}{2m} \right) C(c_v, c_w)$$

where k_v and k_w are the degree between each pair of nodes v and w ($v \neq w$), A_{vw} is the presence/absence of an edge that links nodes v and w , $2m$ corresponds to the sum of all edges in the network, and $C(c_v, c_w)$ is 1 if nodes v and w belong to the same module or 0 if not.

Rich Clubs. The rich club coefficient, $\phi(k)$, is defined below [36]. For each degree k , it computes the density of the sub-network comprised of nodes with degree higher than k , where $E_{>k}$ is the number of edges with degree higher than k and $N_{>k}$ is the number of nodes with degree higher than k . If for some k close to k_{max} , $\phi(k) \rightarrow 1$, then a rich club is said to be present. Others argued that since the rich club coefficient is a monotonically increasing function, even for networks that aren't related, this metric as is may be misleading [37]. Hence, they proposed to normalize the rich-club coefficient against a null-model with the same degree distribution, $\rho(k)$:

$$\phi(k) = \frac{2E_{>k}}{N_{>k}(N_{>k}-1)} \quad \rho(k) = \frac{\phi(k)}{\phi_{null}(k)}$$

If for some k close to k_{max} , $\rho(k) > 1$, then a rich club is said to be present with respect to the null case.

Participation Coefficient. The Participation Coefficient, PC , of node i is:

$$PC(i) = 1 - \sum_{s=1}^{N_m} \left(\frac{k_{is}}{k_i} \right)^2$$

where k_i is the degree of i and k_{is} is the number of links from i to nodes in community s . We used this definition to study whether nodes in the rich club have links uniformly distributed among all communities ($PC(i)$ close to 1) or if all its links are within its own community ($PC(i)$ close to 0).

Within-module Degree. The within-module Degree z-score of node i is :

$$z_i = \frac{k_i(m_i) - \langle k_i(m_i) \rangle}{\sigma^{k(m_i)}}$$

where m_i is the module containing node i , $k_i(m_i)$ is the within-module degree of i , and $\langle k_i(m_i) \rangle$ and $\sigma^{k(m_i)}$ are the respective mean and standard deviation of the within-module m_i degree distribution.

Code Availability. Our source code is publicly available at <https://github.com/jomy-kk/fMRI-EEG-brainConnectome>.

Brain visualization. Whole-brain images were produced by MATLAB BrainNet Viewer 1.7 [38]. Margin snippets are from the Gray's atlas.

ACKNOWLEDGMENTS

We would like to thank Francisca Ayres Ribeiro for helping us with the datasets with most of the pre-processing done, that are part of the project [32]. Thanks to Prof. Patrícia Figueiredo and Prof. Alexandre Francisco who got us in touch with Francisca.

REFERENCES

- [1] Bullmore, E. T. & Bassett, D. S. Brain Graphs: Graphical Models of the Human Brain Connectome. *Annu. Rev. Clin. Psychol.* **7**, 113–140 (2011).
- [2] Farahani, F. V., Karwowski, W. & Lighthall, N. R. Application of Graph Theory for Identifying Connectivity Patterns in Human Brain Networks: A Systematic Review. *Front. Neurosci.* **13**, 585 (2019).
- [3] Bullmore, E. & Sporns, O. Complex brain networks: graph theoretical analysis of structural and functional systems. *Nat. Rev. Neurosci.* **10**, 186–198 (2009).
- [4] Achard, S., Salvador, R., Whitcher, B., Suckling, J. & Bullmore, E. A Resilient, Low-Frequency, Small-World Human Brain Functional Network with Highly Connected Association Cortical Hubs. *J. Neurosci.* **26**, 63–72 (2006).
- [5] Meunier, D., Lambiotte, R. & Bullmore, E. T. Modular and Hierarchically Modular Organization of Brain Networks. *Front. Neurosci.* **4** (2010).
- [6] Ferrarini, L. *et al.* Hierarchical functional modularity in the resting-state human brain. *Hum. Brain Mapp.* **30**, 2220–2231 (2009).
- [7] van den Heuvel, M. P. & Sporns, O. Rich-Club Organization of the Human Connectome. *J. Neurosci.* **31**, 15775–15786 (2011).
- [8] Rubinov, M. & Sporns, O. Complex network measures of brain connectivity: Uses and interpretations. *NeuroImage* **52**, 1059–1069 (2010).
- [9] Tononi, G., Sporns, O. & Edelman, G. M. A measure for brain complexity: relating functional segregation and integration in the nervous system. *Proc. Natl. Acad. Sci.* **91**, 5033–5037 (1994).
- [10] Cohen, J. R. & D’Esposito, M. The Segregation and Integration of Distinct Brain Networks and Their Relationship to Cognition. *J. Neurosci.* **36**, 12083–12094 (2016).
- [11] He, B. (ed.) *Neural engineering* (Springer, New York, 2013), second edition edn.
- [12] Erdos, P. & Renyi, A. On the evolution of random graphs. *Publ. Math. Inst. Hungary. Acad. Sci.* **5**, 17–61 (1960).
- [13] Watts, D. J. & Strogatz, S. H. Collective dynamics of ‘small-world’ networks. *Nat.* **393**, 440–442 (1998).
- [14] Sporns, O. & Honey, C. J. Small worlds inside big brains. *Proc. Natl. Acad. Sci.* **103**, 19219–19220 (2006).
- [15] Schomer, D. L. & Lopes da Silva, F. H. *Niedermeyer’s electroencephalography: basic principles, clinical applications, and related fields* (2018).
- [16] Laufs, H. *et al.* Electroencephalographic signatures of attentional and cognitive default modes in spontaneous brain activity fluctuations at rest. *Proc. Natl. Acad. Sci.* **100**, 11053–11058 (2003).
- [17] Buckner, R. L., Andrews-Hanna, J. R. & Schacter, D. L. *The Brain’s Default Network: Anatomy, Function, and Relevance to Disease*. *Annals New York Acad. Sci.* **1124**, 1–38 (2008).
- [18] Andrews-Hanna, J. R., Smallwood, J. & Spreng, R. N. The default network and self-generated thought: component processes, dynamic control, and clinical relevance: The brain’s default network. *Annals New York Acad. Sci.* **1316**, 29–52 (2014).
- [19] Nielsen, F., Balslev, D. & Hansen, L. K. Mining the posterior cingulate: Segregation between memory and pain components. *NeuroImage* **27**, 520–532 (2005).
- [20] The brain from top to bottom - can states of consciousness be mapped in the brain? URL https://thebrain.mcgill.ca/flash/i/i_12/i_12_cr/i_12_cr_con/i_12_cr_con.html.
- [21] Vijayaraghavan, L. *et al.* A selective role for right insula—basal ganglia circuits in appetitive stimulus processing. *Soc. Cogn. Affect. Neurosci.* **8**, 813–819 (2013).
- [22] Girvan, M. & Newman, M. E. J. Community structure in social and biological networks. *Proc. Natl. Acad. Sci.* **99**, 7821–7826 (2002).
- [23] Blondel, V. D., Guillaume, J.-L., Lambiotte, R. & Lefebvre, E. Fast unfolding of communities in large networks. *J. Stat. Mech. Theory Exp.* **2008**, P10008 (2008).
- [24] Reichardt, J. & Bornholdt, S. Statistical mechanics of community detection. *Phys. Rev. E* **74**, 016110 (2006).
- [25] Pons, P. & Latapy, M. Computing Communities in Large Networks Using Random Walks. vol. 3733, 284–293 (Springer Berlin Heidelberg, Berlin, Heidelberg, 2005).
- [26] Rosvall, M. & Bergstrom, C. T. Maps of random walks on complex networks reveal community structure. *Proc. Natl. Acad. Sci.* **105**, 1118–1123 (2008).
- [27] Guimerà, R. & Nunes Amaral, L. A. Functional cartography of complex metabolic networks. *Nat.* **433**, 895–900 (2005).

- [28] Rizkallah, J. *et al.* Decreased integration of EEG source-space networks in disorders of consciousness. *NeuroImage: Clin.* **23**, 101841 (2019).
- [29] Power, J., Schlaggar, B., Lessov-Schlaggar, C. & Petersen, S. Evidence for Hubs in Human Functional Brain Networks. *Neuron* **79**, 798–813 (2013).
- [30] Crossley, N. A. *et al.* Cognitive relevance of the community structure of the human brain functional coactivation network. *Proc. Natl. Acad. Sci.* **110**, 11583–11588 (2013).
- [31] Vatansever, D., Menon, D. K., Manktelow, A. E., Sahakian, B. J. & Stamatakis, E. A. Default Mode Dynamics for Global Functional Integration. *J. Neurosci.* **35**, 15254–15262 (2015).
- [32] Wirsich, J. *et al.* EEG and fMRI connectomes are reliably related: a simultaneous EEG-fMRI study from 1.5T to 7T. Tech. Rep., Neuroscience (2020).
- [33] Desikan, R. S. *et al.* An automated labeling system for subdividing the human cerebral cortex on MRI scans into gyral based regions of interest. *NeuroImage* **31**, 968–980 (2006).
- [34] Bastos, A. M. & Schoffelen, J.-M. A Tutorial Review of Functional Connectivity Analysis Methods and Their Interpretational Pitfalls. *Front. Syst. Neurosci.* **9** (2016).
- [35] Newman, M. E. J. Fast algorithm for detecting community structure in networks. *Phys. Rev. E* **69**, 066133 (2004).
- [36] Zhou, S. & Mondragon, R. The Rich-Club Phenomenon in the Internet Topology. *Commun. Lett. IEEE* **8**, 180 – 182 (2004).
- [37] Colizza, V., Flammini, A., Serrano, M. & Vespignani, A. Detecting rich-club ordering in complex networks. *Nat Phys* **2** (2006).
- [38] Brainnet viewer: A network visualization tool for human brain connectomics. plos one 8: e68910.